JOURNAL OF MAGNETIC RESONANCE, Series A **122,** 81–84 (1996)
ARTICLE NO. 0180

Suppression of Cycling Sidebands Using Bi-level Adiabatic Decoupling

ĒRIKS KUPČE,* RAY FREEMAN,† GERHARD WIDER,‡ AND KURT WÜTHRICH‡

*Varian NMR Instruments, 28 Manor Road, Walton-on-Thames, Surrey KT12 2QF, England; †Department of Chemistry, Cambridge University, Lensfield Road, Cambridge CB2 1EW, England; and ‡Institut für Molekularbiologie und Biophysik, ETH Hönggerberg, CH-8093 Zürich, Switzerland

Received June 20, 1996

Repetitive heteronuclear decoupling schemes are susceptible to the problem of cycling sidebands (*1*). Viewed in the time domain, decoupling is basically a repeated refocusing of the divergence of magnetization vectors due to the spin–spin coupling, and unless the focusing is precise and the sampling of the observed signal is exactly synchronized with the focus points, spurious modulation is normally introduced into the free induction decay. The Fourier transform of these oscillatory artifacts consists of pairs of modulation sidebands flanking the resonance frequency and separated from it by the cycling frequency. These cycling sidebands are undesirable because they can eventually interfere with the detection of meaningful NMR signals, for example, the cross peaks in two-dimensional NOESY spectra. In general, the cycling sideband problem is more serious at low decoupler power, which is the preferred operating condition.

Now that efficient adiabatic decoupling schemes have been developed (*2–14*), it is possible to cover chemical-shift ranges that far exceed even those required for carbon-13 decoupling in a field of 18.8 T. Consequently, radiofrequency heating is no longer a serious problem, but some care must be taken to minimize cycling sidebands. We distinguish two main types—*principal* cycling sidebands that occur at frequency offsets of $\pm 1/(T)$ hertz, where T is the adiabatic pulse duration, and *subharmonic* sidebands which appear at $\pm 1/(2T)$ hertz.

The variation of the principal cycling sidebands as a function of the decoupler sweep (Fig. 1) shows a progressive change of phase through almost $\pm 180°$ from one edge of the sweep to the other, but if the sweep direction is reversed, the dispersion contributions are inverted. Averaging over both sweep directions leaves these sidebands everywhere in pure absorption (Fig. 1c). Clearly, the principal sidebands are most prominent for spins resonating near the center of the adiabatic sweep, with weaker, inverted sidebands at the edges, and with nulls at approximately $\frac{1}{4}$ and $\frac{3}{4}$ of the sweep width. This can be understood by considering a two-spin system, IS, in which the S-spin response is represented by two vectors (α and β) arising from the coupling J_{IS}. The vectors α and β diverge at an angular rate $\pm \pi J_{IS}$ rad s^{-1} and begin to reconverge when adiabatic inversion of the I spins interchanges the α and β labels. For I spins at resonance near the center of the sweep, the adiabatic pulse causes reconvergence after a time period of approximately $0.5T$, i.e., near the end of the sweep. They reach full divergence again near the center of the next adiabatic sweep, ready for refocusing. Consequently, these principal sidebands are most intense for spins with chemical shifts near the middle of the sweep.

The subharmonic sidebands also have a phase gradient that is a function of the decoupler sweep, and which is canceled by alternating the sweep direction (Fig. 2). However, these sidebands are most prominent near the edges of the sweep. For a chemical shift near one edge, the corresponding vectors α and β diverge for almost the entire sweep duration T and reconverge to a focus near $2T$, at which time the next adiabatic sweep can have little effect. We must wait until $3T$ for full divergence before spin inversion is once again effective. The resulting modulation frequency is $1/(2T)$ hertz.

The principal and subharmonic sidebands cannot be canceled by simply desynchronizing the decoupling and sampling operations; this only spreads the sidebands across the entire decoupling bandwidth. [The asynchronous decoupling proposed for homonuclear systems (*15*) addresses a different problem, i.e., the artifacts created by the presence of a modulated radiofrequency field (*16*).] Two different procedures are recommended for suppression of the two types of sidebands. Subharmonic sidebands are greatly attenuated by ensuring that spins at all chemical shifts experience the adiabatic spin inversion as nearly as possible at the same time. This suggests the use of *shorter* adiabatic sweeps interspersed with ''windows'' of zero decoupler intensity, implying operation at a higher peak decoupler level, $B_2(\max)$. The use of a low duty cycle (the fraction of the total time for which the decoupler is on) ensures that the power dissipation remains low. Note that for a given $B_2(\max)$, a linear frequency sweep involves the shortest possible sweep duration and therefore the weakest subharmonic sidebands. The intensity of the subharmonic sidebands decreases rapidly as the duty cycle is reduced; for a 50% duty cycle, the principal and the subharmonic sidebands have comparable intensities,

1064-1858/96 $18.00
Copyright © 1996 by Academic Press, Inc.
All rights of reproduction in any form reserved.

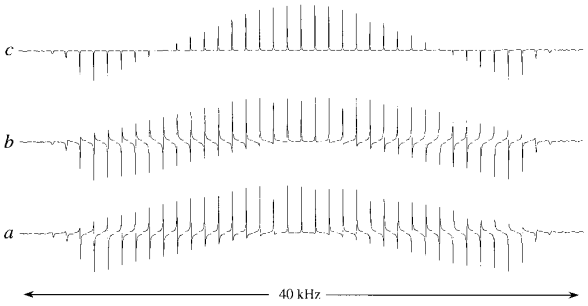

FIG. 1. Low-field principal cycling sidebands at 454 Hz ($T = 2.2$ ms) of the S spin of an IS spin system as a function of offset from the center of the adiabatic frequency sweep (WURST-40). The decoupler offset was incremented in 1 kHz steps over a 40 kHz band. (a) Forward sweep. (b) Reverse sweep. (c) Average of (a) and (b).

whereas for a 25% duty cycle, the subharmonic sidebands virtually disappear.

For the suppression of the principal sidebands it is useful to consider the spurious modulation of the S-spin signal in the time domain (Fig. 3). Suppression can be achieved by averaging n (or a multiple of n) successive S-spin free induction decays recorded with different initial delays $\tau_L = Tk/n$ of the onset of this modulation. Typically k runs from zero to $n - 1$. This procedure entails ''locking'' the system for the short period τ_L in a condition where cycling modulation is negligible. Ideally, a refocusing scheme could be employed during τ_L, with a single short inversion pulse at the midpoint. In practice we use a bi-level decoupling scheme in which the decoupler is at such a high level during τ_L that modulation effects can be neglected until the decoupler is returned to its normal low level for the remainder of the acquisition time. The increasing delay of the onset of the cycling modulation is illustrated in Figs. 3b through 3e. For the purposes of this illustration $n = 4$ and k runs from 0 to 4; in the experiments described below $n = 8$. Averaging over a complete set cancels this modulation and therefore suppresses the principal cycling sidebands.

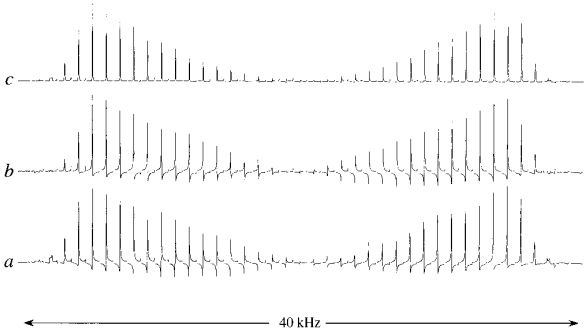

FIG. 2. Subharmonic cycling sidebands at 227 Hz from the experiment of Fig. 1. (a) Forward sweep. (b) Reverse sweep. (c) Average of (a) and (b).

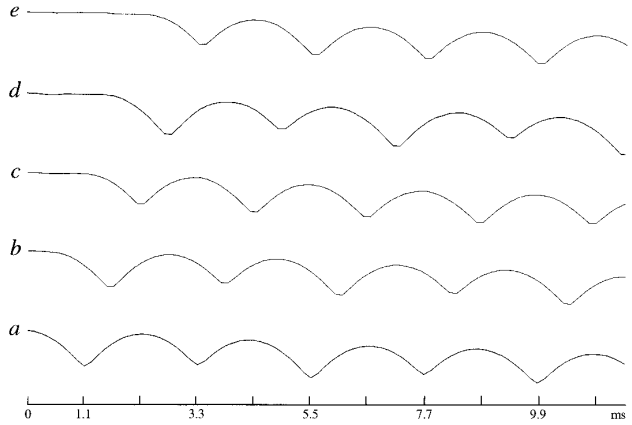

FIG. 3. Modulation of the S-spin free induction signal ''on resonance'' during the bi-level decoupler scheme (see text). The onset of modulation was delayed by operating the decoupler at a higher level during a variable period $\tau_L = Tk/n$, with $T = 2.2$ ms, $n = 4$, and (a) $k = 0$, (b) $k = 1$, (c) $k = 2$, (d) $k = 3$, and (e) $k = 4$. Constant adiabaticity WURST-2 pulses (9) at a level of 10.5 kHz were used for the high-level decoupling; WURST-12 pulses with $\gamma B_2(\max)/2\pi = 6.2$ kHz and a 27.3% duty cycle were used for low-level decoupling, which is equivalent to $\gamma B_2(\mathrm{rms})/2\pi = 2.7$ kHz.

Experiments were carried out to test this scheme by observing protons decoupled from ^{13}C in enriched methyl iodide. Decoupling and acquisition were preceded by a 90° purge pulse on ^{13}C to remove antiphase proton responses. (This precaution can be important in, for example, heteronuclear multiple-quantum correlation experiments with systems containing a range of different values of the spin–spin couplings, and where any choice of the refocusing delay

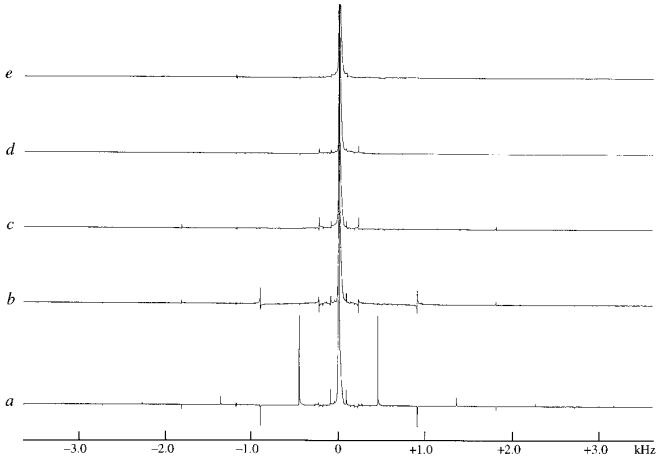

FIG. 4. Progressive attenuation of cycling sidebands by averaging traces of the type shown in Fig. 3. (a) Single trace ($k = 0$), (b) 2 traces ($k = 0, 1$), (c) 4 traces ($k = 0$ to 3), (d) 8 traces ($k = 0$ to 7), and (e) 16 traces ($k = 0$ to 15). Note that in the upper traces the principal sidebands and their higher harmonics are very effectively suppressed, and that the inner sidebands arising from the five-step supercycle are also attenuated. In trace (a) the most intense sidebands are 2.8% of the height of the central peak.

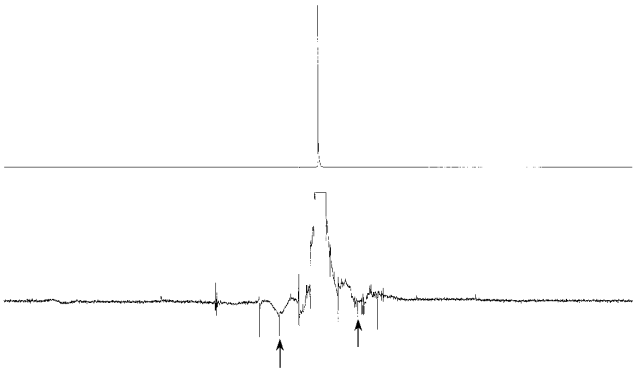

FIG. 5. Cycling sidebands observed under the experimental conditions of Fig. 4e. The 500-fold vertical expansion of the lower trace shows that all the residual sidebands are now less than 0.05% of the height of the main peak. The principal sidebands are indicated by arrows.

leaves antiphase proton components.) During the initial ''locking'' period τ_L, the peak decoupler level was $\gamma B_2(\max)/2\pi = 9.2$ kHz with a duty cycle of unity (no windows). The WURST-2 decoupling scheme was employed with $T = 2.2$ ms and an optimized sweep rate (9). This is equivalent in power dissipation to a constant decoupler level $\gamma B_2(\mathrm{rms})/2\pi = 5.6$ kHz. The first period T was divided into $n = 8$ equal time segments of 275 μs each, and high-level decoupling was imposed for k segments. For the remainder of the acquisition period, low-level decoupling was implemented by a windowed WURST-12 adiabatic sweep with a duty cycle of 27.3%. Although the peak decoupler level was relatively high [$\gamma B_2(\max)/2\pi = 6.2$ kHz], the average power was only equivalent to a constant radiofrequency level $\gamma B_2(\mathrm{rms})/2\pi = 2.7$ kHz. In this manner the bi-level decoupling shifts the onset of the cycling modulation, and the level of the principal cycling sidebands is progressively attenuated as the number of steps k is increased. Increments up to $k = 15$ were used (Fig. 4), spanning a period $2T$; note that under these conditions windowing might not be strictly necessary.

Figure 5 was obtained with the experimental conditions used for Fig. 4e; it includes a 500-fold vertical expansion to show that all the cycling sidebands have been reduced to less than 0.05% of the intensity of the decoupled resonance. There is also some collateral suppression of the *inner* cycling sidebands which arise from the weaker modulation by the five-step phase cycle, because, with k running from 0 to 15, the locking periods τ_L were long enough to allow partial cancellation of time-shifted components. The weak, low-frequency sinusoidal oscillation in the baseline is attributable to the slight perturbation of the proton signal during τ_L.

The decoupling scheme used for the experiments of Figs. 3 through 5, ECO-WURST, eliminates cycling oscillations and cleans up the baselines of decoupled spectra. A stringent test of spectral purity is to record clean ^{13}C- and ^{15}N-decou-

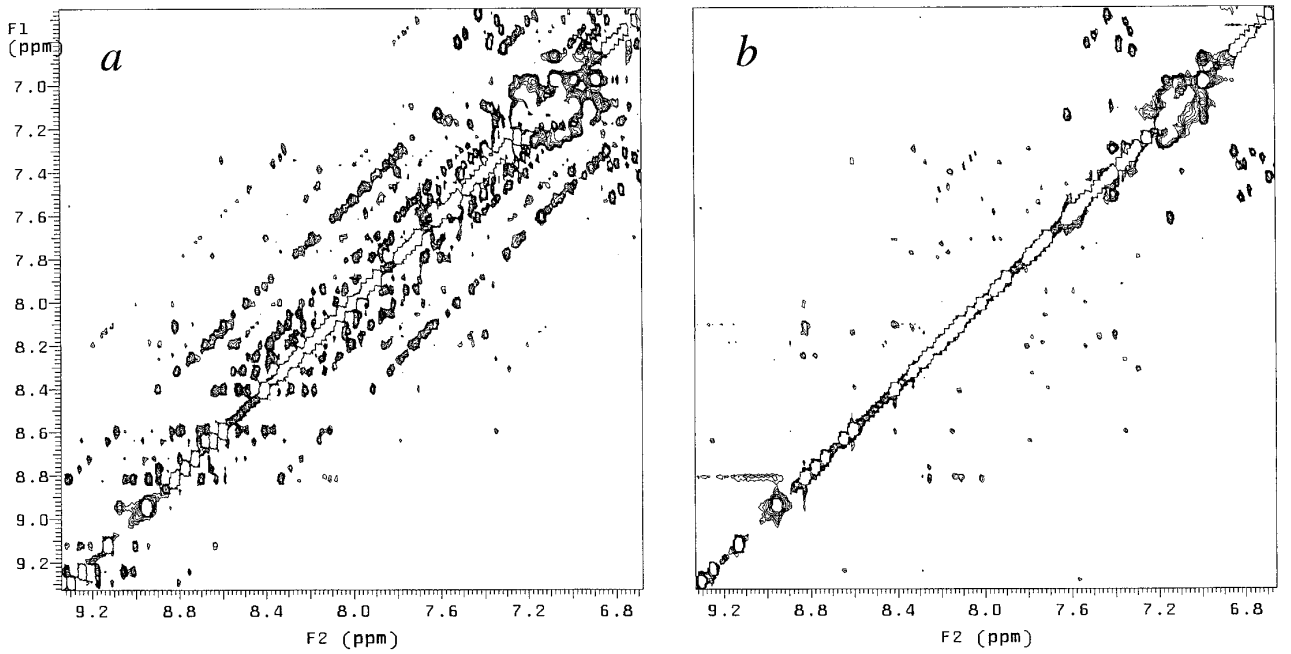

FIG. 6. Comparison of two-dimensional 750 MHz proton NOESY spectra of the uniformly ^{13}C,^{15}N doubly labeled protein 434(1–63). The protein concentration was 2 mM in 90% H_2O/10% D_2O, at pH 4.8 and 15°C. The mixing time was 15 ms, the time-domain data size was 1024 × 512 complex points, the weighting used a cosine^2 function, $t_1(\max) = 65$ ms, and $t_2(\max) = 130$ ms. (a) GARP decoupling of ^{13}C and ^{15}N. (b) ECO-WURST decoupling under equivalent conditions. Lowest contour level was 0.1%.

TABLE 1
ECO-WURST Decoupling Parameters[a] Used in the Experiment of Fig. 6b

Nucleus	Level	Shape index (n)	γB_2(max)/2π (kHz)	γB_2(rms)/2π (kHz)	Duty cycle (%)	τ_L (ms)	T (ms)
^{13}C	High	2	11.6	7.1	100	$3k/8^b$	—
^{13}C	Low	20	5.0	2.5	30	—	3.0[c]
^{15}N	High	2	5.8	3.6	100	$3k/8^b$	—
^{15}N	Low	2	2.5	0.9	30	—	3.0[d]

[a] The adiabaticity factor Q was equal to 2.8 throughout.
[b] k is an integer running between 0 and 15.
[c] This implies the average value of $(J_{CH}T)^{-1} = 2.2$.
[d] This implies the average value of $(J_{NH}\ T)^{-1} = 3.5$.

pled two-dimensional proton–proton Overhauser (NOESY) spectra of a uniformly ^{13}C, ^{15}N doubly labeled protein, where the unambiguous detection of weak cross peaks is essential for structure determination. Simultaneous broadband decoupling of both heteronuclear species puts severe demands on decoupling efficiency and requires effective suppression of cycling sidebands.

Figure 6 compares the experimental results obtained with conventional GARP decoupling (*17*) and with ECO-WURST. It shows the region containing the resonances of the amide and aromatic protons of the two-dimensional 750 MHz proton NOESY spectrum (*18*) of the N-terminal 63-residue DNA-binding domain of the 434 repressor, 434(1–63). The protein was uniformly labeled with ^{13}C and ^{15}N. Equivalent conditions of decoupler power dissipation were used in both experiments. The five-step phase cycle (0°, 150°, 60°, 150°, 0°) of Tycko *et al.* (*19*) was used. The GARP scheme used $\gamma_C B_2/2\pi = 2.5$ kHz for ^{13}C decoupling (~12.5 kHz bandwidth) and $\gamma_N B_2/2\pi = 0.9$ kHz for ^{15}N decoupling (~4.5 kHz bandwidth). The experimental parameters for ECO-WURST are listed in Table 1. The combination of poorly suppressed cycling sidebands and incompletely decoupled ^{13}C and ^{15}N splittings makes the spectrum of Fig. 6a virtually useless for the detection of weak NOESY cross peaks close to the diagonal, whereas the ECO-WURST scheme provides a clear record of these important correlations (Fig. 6b).

Cycling sidebands could be minimized by operation at high decoupler power, but this would conflict with the goal of achieving the desired decoupling bandwidth with the lowest possible sample heating. We show that even at low decoupler power, the subharmonic cycling sidebands are effectively suppressed by employing a windowed WURST sequence designed to invert all I spins at about the same time, irrespective of their chemical shifts. The principal cycling sidebands are suppressed by introducing a progressive time shift of the cycling modulation, followed by averaging of the resulting free induction decays. This bi-level decoupling scheme also reduces the subharmonic sidebands. The ''inner sidebands,'' related to the (slower) repetition rate of the five-step supercycle (*19*), are reduced to a very low level by taking care to satisfy the adiabatic condition ($Q = 2.8$ in these experiments). With these precautions, all sidebands are held below 0.05% of the intensity of the decoupled line, and the residuals are mainly attributable to subtraction errors due to instrument instabilities. The ECO-WURST scheme permits the detection of weak cross peaks in multidimensional ^{1}H-detected NMR experiments on ^{13}C- and ^{15}N-labeled compounds, and could also be used in experiments with other nuclei, for example, ^{31}P, ^{19}F, or ^{2}H.

REFERENCES

1. A. J. Shaka, P. B. Barker, C. J. Bauer, and R. Freeman, *J. Magn. Reson.* 67, 396 (1986).
2. T. Fujiwara, T. Anai, N. Kurihara, and K. Nagayama, *J. Magn. Reson. A* 104, 103 (1993).
3. Z. Starčuk, Jr., K. Bartušek, and Z. Starčuk, *J. Magn. Reson. A* 107, 24 (1994).
4. M. R. Bendall, *J. Magn. Reson. A* 112, 126 (1995).
5. E. Kupče and R. Freeman, *J. Magn. Reson. A* 115, 273 (1995).
6. R. Fu and G. Bodenhausen, *Chem. Phys. Lett.* 245, 415 (1995).
7. E. Kupče and R. Freeman, *J. Magn. Reson. A* 117, 246 (1995).
8. R. Fu and G. Bodenhausen, *J. Magn. Reson. A* 117, 324 (1995).
9. E. Kupče and R. Freeman, *J. Magn. Reson. A* 118, 299 (1996).
10. R. Fu and G. Bodenhausen, *J. Magn. Reson. A* 119, 129 (1996).
11. E. Kupče and R. Freeman, *Chem. Phys. Lett.* 250, 523 (1996).
12. A. Tannús and M. Garwood, *J. Magn. Reson. A* 120, 133 (1996).
13. E. Kupče, R. Freeman, G. Wider, and K. Wüthrich, *J. Magn. Reson. A* 120, 264 (1996).
14. J. Baum, R. Tycko, and A. Pines, *Phys. Rev. A* 32, 3435 (1985).
15. J. Weigelt, A., Hammarström, W. Bermel, and G. Otting, *J. Magn. Reson. B* 110, 219 (1996).
16. F. Bloch and A. Siegert, *Phys. Rev.* 57, 522 (1940).
17. A. J. Shaka, P. B. Barker, and R. Freeman, *J. Magn. Reson.* 64, 547 (1985).
18. D. Neri, G. Wider, and K. Wüthrich, *FEBS Lett.* 303, 129 (1992).
19. R. Tycko, A. Pines, and R. Gluckenheimer, *J. Chem. Phys.* 83, 2775 (1985).